Title
Benzoquinonoid-bridged dinuclear actinide complexes

Journal
Dalton Transactions, 46(35)

ISSN
1477-9226

Authors
Hohloch, Stephan
Pankhurst, James R
Jaekel, Esther E
et al.

Publication Date
2017-09-12

DOI
10.1039/c7dt02728a

Peer reviewed

Benzoquinonoid-bridged dinuclear actinide complexes

Stephan Hohloch,[a,b,c †] James R. Pankhurst,[a,b,d †] Esther E. Jaekel,[a] Bernard F. Parker,[a,b] Daniel J. Lussier,[a,b] Mary E. Garner,[a,b] Corwin H. Booth,[b] Jason B. Love[d] and John Arnold[a,b]*

Received 00th January 20xx,
Accepted 00th January 20xx

DOI: 10.1039/x0xx00000x

www.rsc.org/

We report the coordination chemistry of the tripodal tris[2-amido(2-pyridyl)ethyl]amine ligand, **L**, with thorium(IV) and uranium(IV). Using a salt-metathesis strategy from the potassium salt of this ligand, **K_3L**, new actinide complexes were isolated, namely the dimeric thorium complex $[ThCl(L)]_2$ (**1**) and the monomeric uranium complex UI(THF)(L) (**2**); under different crystallisation conditions, the dimeric uranium complex is also isolated, $[UI(L)]_2$ (**2-dimer**). With the aim of studying electronic phenomena such as magnetic exchange between two actinide ions, we have synthesised the first examples of dinuclear, quinoid-bridged actinide complexes from dianionic 2,5-bis[2,6-(diisopropyl)anilide]-1,4-benzoquinone ($\mathbf{Q^{Dipp}}$) and 2,5-bis[2-(methoxy)anilide]-1,4-benzoquinone ($\mathbf{Q^{OMe}}$) ligands. The resulting complexes are $[Th(L)]_2Q^{Dipp}$ (**3**), $[Th(THF)(L)]_2Q^{OMe}$ (**5**) and $[U(L)]_2Q^{OMe}$ (**6**). The targeted $[U(L)]_2Q^{Dipp}$ complex (**4**) could not be isolated. All isolated complexes have been characterised by spectroscopic methods and X-ray crystallography. The uranium(IV) complexes **2-dimer** and **6** have been studied by SQUID magnetometry but indicate that there is negligible magnetic exchange between the two uranium(IV) ions. The reduced form of **6**, [K(18-c-6)][$\mathbf{6}^-$] is unstable and highly sensitive, but X-ray crystallography indicates that it is a novel $U^{IV}U^{IV}$ complex bridged by a quinoid-radical.

Introduction

Bridging quinoid ligands have been used extensively in transition metal chemistry[1] to study properties such as electron transfer,[2] spin-spin coupling,[3] mixed valency,[4] valence tautomerism[5] and single-molecule magnetism (SMM).[6] Donor atoms are included in the extended π-conjugation of quinoid ligands, which makes this ligand class well suited to studying intermetallic communication. Moreover, quinoid ligands are highly tuneable (see Scheme 1: X = H, halide or nitro; Ar = aromatic imino substituent) and it has been shown that varying the substituents or the donor atoms on the quinoid ligand has a strong influence on the electronic properties of the resulting dinuclear bridged complexes. For example, an [O,N,O,N]-quinoid ligand has been shown to promote stronger anti-ferromagnetic coupling between two copper(II) ions compared to its isoelectronic [O,O,O,O]-quinoid analogue.[3] Owing to their redox-activity, radical-bridged complexes can also be prepared using quinoid ligands.[7] In one such example, much stronger antiferromagnetic exchange was demonstrated between iron(II) centres when the quinoid bridge was radical in comparison with the neutral analogue ($J \lesssim -900$ cm^{-1} for the radical; $J = -2.9$ cm^{-1} for the neutral complex).[6]

In contrast to transition metal chemistry, the use of bridging benzoquinonoids in bimetallic *f*-element chemistry is unexplored. Low-oxidation-state uranium complexes bearing other redox-active ligands such as pyridine di-imines, 2,2'-bipyridines, Schiff-bases, α-di-imines, amido-phenolates and dioxophenox-azines form complexes of ligand-centred radicals from redox reactions.[8] Dinuclear lanthanide complexes bridged by redox-active ligands such as dinitrogen,[9] tetra(pyridyl)pyrazine,[10] indigo[11] and bi(pyridyl)tetrazine[12] have been shown to display strong magnetic exchange and SMM behaviour. Furthermore, SMM has been observed for dinuclear lanthanide complexes bearing radical tetrathiafulvalene[13] and quinone-tetrathiafulvalene ligands,[14] although strong inter-metallic magnetic exchange was not observed in those cases. It is therefore surprising that similar actinide complexes of bridging quinoid ligands have not yet been reported, as uranium single-molecule magnets have been a focal point of recent research.[15] Multinuclear uranium complexes containing bridging ligands have often displayed varying degrees of electronic or magnetic intermetallic coupling. To give a few illustrative examples: dinuclear uranium(V) complexes containing chalcogenide bridges show anti-ferromagnetic coupling around 20 K,[16] but magnetic coupling in related uranium(IV) complexes was less distinct;[17] an inverse-sandwich complex with a μ_2-η^6:η^6-arene ligand bridging two uranium(III) centres is thought to display SMM behaviour at 1.8 K;[18] two uranium(V) centres linked by a bis-imido ligand undergoes anti-ferromagnetic coupling between 5 and 40 K;[19] and weak

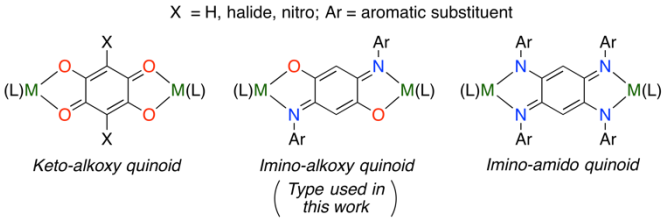

Scheme 1. General depiction of previously reported, dinuclear quinoid-bridged transition metal complexes, highlighting the variety of donor atoms, donor-atom substituents and quinoid substituents that can be incorporated. See references 1–7.

[a] *Department of Chemistry, University of California, Berkeley, California 94720, United States. Email: arnold@berkeley.edu*
[b] *Chemical Sciences Division, Lawrence Berkeley National Laboratory, Berkeley, California, 94720, United States*
[c] *Department of Chemistry, University of Paderborn, Warburger Straße 100, 33098 Paderborn, Germany*
[d] *EaStCHEM School of Chemistry, The University of Edinburgh, Joseph Black Building, David Brewster Road, Edinburgh, EH9 3FJ, United Kingdom*
†These authors contributed equally to the work.
Electronic Supplementary Information (ESI) available: all spectroscopic, crystallographic, voltammetric, magnetometric and computational data are given along with instrumentation details. See DOI: 10.1039/x0xx00000x

ferromagnetic communication is present in di- and tri-nuclear uranium(IV) arylacetylide complexes.[20]

Tripodal ligands have been used extensively in transition metal quinoid chemistry to impart kinetic and thermodynamic stability on the resulting bimetallic complexes, and also because of the well-defined volume of the coordination sphere that is available to introduce the bridging quinoid ligand. For similar reasons, these multidentate ligands have also been employed for similar reasons to study novel modes of bonding, reactivity and electronic structure. In this regard, significant advances in actinide chemistry have come by use of substituted tris(2-aminoethyl)amine ligands (tren),[21] triazacyclononane ligands (tacn),[16b, 22] and tripodal phosphino-amido-amine ligands.[23]

Here we describe the synthesis of the first dinuclear actinide complexes of the tripodal tris[2-amino(2-pyridyl)-ethyl]amine ligand. By incorporating two different bridging [O,N,O,N]-quinoid ligands bearing either *ortho*-anisyl or di-isopropylphenyl (Dipp) imino-substituents we can also report the first examples of quinoid-bridged dinuclear actinide complexes. We have studied these compounds using cyclic voltammetry and magnetometry, and we also report our attempts to isolate a rare quinoid-radical-bridged $U^{IV}U^{IV}$ complex.

Experimental section

Caution! Depleted uranium (primary isotope ^{238}U) and natural thorium (primary isotope ^{232}Th) are both weak α-emitters (4.197 and 4.012 MeV, respectively) with half-lives of 4.47×10^9 and 1.41×10^{10} years, respectively; manipulations and reactions should be carried out in monitored fume hoods or an inert-atmosphere drybox in a radiation laboratory equipped with α- and β-counting equipment.

Cyclic voltammograms were recorded with a three-electrode system, using a Pt disc working-electrode, Pt mesh counter-electrode and Ag wire quasi-reference electrode. A 1 mM solution of the analyte was employed using 0.1 M THF solution of $[^nBu_4N][PF_6]$ as the supporting electrolyte. Potentials were referenced against the ferrocenium/ferrocene redox couple (E, Fc^+/Fc = 0 V). Magnetic susceptibility measurements were performed using Quantum Design MPMS (for **2-dimer**) and MPMS2 (for **6**) SQUID magnetometers. DC magnetic susceptibility measurements were performed at temperatures ranging from 2-300 K under applied DC fields of 1000 Oe (0.1 T), 20,000 Oe (2.0 T), and 70,000 Oe (7.0 T). Magnetic samples were prepared by flame-sealing 14 mg of crystalline powder inside 7 mm quartz tubes.

Details of materials, CCDC numbers and other methods can be found in the Supporting Information.

Synthesis of the ligands

Synthesis of tris[2-amino(2-pyridyl)ethyl]amine, H_3L

Our procedure for the preparation of **H_3L** differs from that published previously.[24] Neat 2-fluoro-pyridine (3.2 eq, 5 g, 51 mmol, 4.5 mL) was mixed under a flow of nitrogen gas with K_2CO_3 (3.2 eq, 7.10 g, 51.5 mmol) and was then heated to 60 °C. Tris(2-aminoethyl)amine, (1 eq, 2.35 g, 16.1 mmol, 2.4 mL) was added dropwise through a rubber septum to the mixture over 10 minutes. The mixture was heated for 1 hour at 60 °C. The temperature was slowly raised to 130 °C and then stirred at this temperature for 3 days. The mixture was then cooled to room temperature and extracted with 100 mL of chloroform. The organic phase was washed with saturated $KHCO_{3(aq)}$ (3 x 20 mL), water (3 x 20 mL) and brine (1 x 20 mL) and then dried over Na_2SO_4 (20 g). The solution was filtered and the solvent was evaporated, producing a yellow oil. Remaining chloroform was removed through trituration with toluene (3 x 30 mL) and the resulting oil was dried under vacuum overnight at room temperature to give **H_3L** as a yellow oil, which slowly solidifies over one or two days. Yield: 5.32 g, 13.8 mmol (86 %). ^1H NMR (500 MHz, CD_3CN, 300 K): δ_H / ppm 2.71 (t, $^3J_{HH}$ = 6.1 Hz, 6H, ethyl-C*H*$_2$), 3.32 (q, $^3J_{HH}$ = 5.9 Hz, 6H, ethyl-C*H*$_2$), 5.29 (s, 3H, N*H*), 6.36 (d, $^3J_{HH}$ = 8.4 Hz, 3H, py *meta-H*), 6.48 (t, $^3J_{HH}$ = 6.1 Hz, 3H, py *meta-H*), 7.32 (t, $^3J_{HH}$ = 6.9 Hz, 3H, py *para-H*), 7.98 (d, $^3J_{HH}$ = 4.1 Hz, 3H, py *ortho-H*). $^{13}C\{^1H\}$ NMR (125 MHz, CD_3CN, 300 K): δ_C / ppm 40.4 (ethyl-*C*H$_2$), 54.3 (ethyl-*C*H$_2$), 108.9 (py *meta-C*), 113.1 (py *meta-C*), 137.8 (py *para-C*), 148.8 (py *ortho-C*), 160.1 (py *ipso-C*).

Synthesis of K_3L

In an oven-dried 500 mL Schlenk flask, **H_3L** (1 eq, 18.5 mmol, 7 g) was dissolved in *ca.* 200 mL toluene. $K[N(SiMe_3)_2]$ (3.1 eq, 57.4 mmol, 11.5g) was added as a solid in 5 portions over 10 minutes to the mixture, forming a thick yellow slurry that was then stirred overnight at room temperature. The yellow solids were isolated by filtration, washed with cold toluene and hexane, and then dried under vacuum for 5 hours. **K_3L** was obtained as a fluffy yellow powder. Yield: 8.6 g, 17.6 mmol (95 %). ^1H NMR (400 MHz, CD_3CN, 300 K): δ_H / ppm 2.69 (t, $^3J_{HH}$ = 4.2 Hz, 6H, ethyl-C*H*$_2$), 3.20 (t, $^3J_{HH}$ = 4.2 Hz, 6H, ethyl-C*H*$_2$), 6.28 – 6.20 (m, 6H, py *meta-H*), 7.21 – 7.18 (m, 3H, py *para-H*), 7.88 – 7.86 (m, 3H, py *ortho-H*). $^{13}C\{^1H\}$ NMR (100 MHz, $CDCl_3$, 300 K): δ_C / ppm 41.7 (ethyl-*C*H$_2$), 54.8 (ethyl-*C*H$_2$), 108.2 (py *meta-C)*, 110.7 (py *meta-C)*, 137.3 (py *para-C)*, 148.8 (py *ortho-C)*, 161.5 (py *ipso-C)*. Elemental analysis calculated for $C_{21}H_{24}N_7K_3$: C, 51.29 %; H, 4.92 %; N, 19.94 %. Found: C, 51.13 %; H, 5.01 %; N, 19.86 %. UV/vis (CH_3CN), λ / nm (ε / $dm^3\ mol^{-1}\ cm^{-1}$): 249 (60,300), 299 (12,500), 359 (1800).

General synthetic procedure for quinones H_2Q^{Dipp} and H_2Q^{OMe}

The amino-quinones (H_2Q^R, R = Dipp or *ortho*-anisyl) were synthesised following the procedure reported by Schweinfurt *et al*.[1d] 2,5-Dihydroxybenzoquinone (1 eq, 6.45 mmol, 900 mg) was suspended in 60 mL of acetic acid at room temperature and the appropriate aniline (2 eq) was added, resulting in a colour change to orange-red. The mixture was heated at 115 °C for 4 hours. The reaction mixture was poured into water (500 mL) and the precipitate was isolated by filtration and air-dried for 1 hour at room temperature. The resulting solids were then dissolved in dichloromethane (100 mL) and stirred over $MgSO_4$ (15 g) for 10 minutes. The H_2Q^R was isolated after filtration and evaporation of the solvent.

Synthesis of H_2Q^{Dipp}

Using 2,6-diisopropylaniline (2 eq, 12.9 mmol, 2.29 g, 2.45 mL). The product was purified by silica gel column chromatography, using CH_2Cl_2/MeOH (99:1) as the eluent, and isolated as a red-pink powder. Yield: 1.18 g, 2.58 mmol (40 %). ^{1}H NMR (500 MHz, $CDCl_3$, 300 K): δ_H / ppm 1.19 (d, $^3J_{HH}$ = 6.8 Hz, 12H, ^{i}Pr-C*H*$_3$), 1.27 (d, $^3J_{HH}$ = 6.8 Hz, 12H, ^{i}Pr-C*H*$_3$), 3.00 (sept, $^3J_{HH}$ = 7.0 Hz, 4H, ^{i}Pr-C*H*), 5.08 (s, 2H, quinone C*H*), 7.28 (d, $^3J_{HH}$ = 8.3 Hz, 4H, Dipp *meta-H*), 7.40 (t, $^3J_{HH}$ = 7.7 Hz, 2H, Dipp *para-H*), 7.68 (s, 2H, N*H*). ^{13}C{^{1}H} NMR (125 MHz, $CDCl_3$, 300 K): δ_C / ppm 23.4 (^{i}Pr-*C*H$_3$), 24.7 (^{i}Pr-*C*H$_3$), 28.7 (^{i}Pr-*C*H), 95.05 (quinone *C*H), 124.2 (Dipp *meta-C*), 129.3 (Dipp *ortho-C*), 131.0 (Dipp *para-C*), 146.3 (Dipp *ipso-C*), 151.7 (quinone *C*N), 179.1 (quinone *C*O). UV/vis (THF), λ / nm (ε / dm^3 mol^{-1} cm^{-1}): 239 (sh, 17,333), 342 (31,000).

Synthesis of H_2Q^{OMe}

Using *ortho*-anisidine (2 eq, 12.9 mmol, 1.59 g, 1.5 mL). The product was obtained as a dark brown microcrystalline solid which required no further purification. Yield: 1.77g, 5.05 mmol (78 %). ^{1}H NMR (600 MHz, $CDCl_3$, 300 K): δ_H / ppm 3.89 (s, 6H, OC*H*$_3$), 6.15 (s, 2H, quinone C*H*), 6.94 (d, $^3J_{HH}$ = 8.16 Hz, 2H, anisidine *meta-H*), 6.99 (t, $^3J_{HH}$ = 7.68 Hz, 2H, anisidine *para-H*), 7.14 (t, $^3J_{HH}$ = 8.04 Hz, 2H, anisidine *meta-H*), 7.39 (d, $^3J_{HH}$ = 7.86 Hz, 2H, anisidine *ortho-H*), 8.46 (s, 2H, N*H*). ^{13}C{^{1}H} NMR (150 MHz, $CDCl_3$, 300 K): δ_C / ppm 55.7 (O*C*H$_3$), 96.3 (quinone *C*H), 111.1 (anisidine *meta-C*), 120.7 (anisidine *para-C*), 121.2 (anisidine *meta-C*), 125.9 (anisidine *ortho-C*), 126.6 (anisidine *ipso-C*N), 145.6 (anisidine *ipso-C*OCH$_3$), 151.5 (quinone *C*N), 180.5 (quinone *C*O). UV/vis (THF), λ / nm (ε / dm^3 mol^{-1} cm^{-1}): 239 (sh, 9000), 266 (10,800), 278 (10,500), 400 (8700).

Synthesis of metal complexes

Synthesis of $[ThCl(L)]_2$ (1)

A solution of $ThCl_4(DME)_2$ (1 eq, 0.5 mmol, 277 mg) in THF (5 mL) was added drop-wise to a stirred yellow solution of **K_3L** (1 eq, 0.5 mmol, 265 mg) in THF (10 mL). The resulting dull yellow suspension was stirred overnight at room temperature. The suspended solids were removed by filtering twice through Celite® and the filtrate was concentrated to approximately 2 mL. The THF solution was layered with hexane and cooled to –40 °C for 5 hours, causing the product to precipitate. The product was isolated as yellow microcrystalline material by decanting the supernatant and drying the solids under vacuum for several hours. Yield: 240 mg, 0.375 mmol (75 %). ^{1}H NMR (500 MHz, d_5-pyridine, 300 K): δ_H / ppm 3.03 (t, $^3J_{HH}$ = 5.8 Hz, 12H, ethyl-C*H*$_2$), 3.40 (t, $^3J_{HH}$ = 5.8 Hz, 12H, ethyl-C*H*$_2$), 5.74 (d, $^3J_{HH}$ = 8.45 Hz, 6H, py *meta-H*), 6.04 (t, $^3J_{HH}$ = 6.1 Hz, 6H, py *meta-H*), 7.03 (t, $^3J_{HH}$ = 6.85 Hz, 6H, py *para-H*), 8.82 (d, $^3J_{HH}$ = 4 Hz, 6H, py *ortho-H*). ^{13}C{^{1}H} NMR (175 MHz, d_5-pyridine, 300 K): δ_C / ppm 46.2 (ethyl-*C*H$_2$), 55.1 (ethyl-*C*H$_2$), 104.1 (py *meta-C*), 107.6 (py *meta-C*), 140.1 (py *para-C*), 146.8 (py *ortho-C*), 168.2 (py *ipso-C*). Elemental analysis calculated for $C_{42}H_{48}N_{14}Cl_2Th_2$: C, 39.29 %; H, 3.77 %; N, 15.27 %. Found: C, 39.15 %; H, 3.86 %; N, 15.03 %. UV/vis (THF), λ / nm (ε / dm^3 mol^{-1} cm^{-1}): 261 (sh, 56,700), 271 (59,500), 363 (9,400).

Synthesis of [UI(THF)(L)] (2)

A solution of UI_4(dioxane)$_2$ (1 eq, 0.5 mmol, 460 mg) in THF (5 mL) was added drop-wise to a stirred yellow solution of **K_3L** (1 eq, 0.5 mmol, 265 mg) in THF (10 mL). The resulting orange-red suspension was stirred overnight at room temperature. The suspended solids were removed from the mixture by filtering twice through Celite® and the THF filtrate was concentrated to approximately 2 mL. The orange solution was then stored at –40 °C for 5 hours to induce the precipitation of **2** as a microcrystalline red-orange powder. The supernatant was removed and the product was dried under vacuum for several hours. Yield: 307 mg, 0.415 mmol (83 %). ^{1}H NMR (500 MHz, d_5-pyridine, 300 K): δ_H / ppm –13.02 (s, 6H, ethyl-C*H*$_2$), 9.26 (s, 3H, py-*H*), 11.18 (s, 3H, py-*H*), 14.62 (s, 3H, py-*H*), 14.76 (s, 6H, ethyl-C*H*$_2$), 17.14 (s, 3H, py-*H*). Elemental analysis calculated for $C_{25}H_{32}N_7O_1I_1U_1$ 0.2THF: C, 37.52 %; H, 4.10 %; N, 11.87 %. Found: C, 37.08 %; H, 4.24 %; N, 10.89 %. UV/vis (THF), λ / nm (ε / dm^3 mol^{-1} cm^{-1}): 250 (46,900), 360 (6500). Evans method magnetic moment: μ_{eff} = 2.85 μ_B.

Synthesis of dinuclear, quinoid-bridged complexes

General procedure

A 5 mL THF solution of the amino-quinone **H_2Q^{Dipp}** or **H_2Q^{OMe}** (1 eq, 0.1 mmol) was prepared and K[N(SiMe$_3$)$_2$] (2 eq, 0.2 mmol, 40 mg) was added to the solution directly as a solid. The resulting brown (**K_2Q^{Dipp}**) or orange (**K_2Q^{OMe}**) mixture was stirred for 1.5 hours at room temperature, during which time a precipitate formed. The resulting suspension was added drop-wise to a THF solution (5 mL) of the appropriate metal precursor (**1** or **2**). The colour changed to red (for reactions involving **1**) or dark brown (for reactions involving **2**) and the suspension was stirred for 18 hours at room temperature. The reaction mixture was then filtered through Celite® and the THF filtrate was concentrated to approximately 5 % of its original volume. Storage of the concentrated solution at –40 °C induced crystallization of the desired complexes in moderate to good yield as microcrystalline solids.

Synthesis of $[Th(L)]_2Q^{Dipp}$ (3)

From **H_2Q^{Dipp}** (1 eq, 46 mg, 0.1 mmol) and **1** (1 eq, 0.1 mmol, 128 mg). Isolated as a microcrystalline red solid. Yield: 58 mg, 0.035 mmol (35 %). ^{1}H NMR (700 MHz, d_5-pyridine, 300 K): δ_H / ppm 1.11 (d, $^3J_{HH}$ = 6.6 Hz, 12H, ^{i}Pr-C*H*$_3$), 1.28 (d, $^3J_{HH}$ = 6.7 Hz, 12H, ^{i}Pr-C*H*$_3$), 2.67 (t, $^3J_{HH}$ = 5.5 Hz, 24H, ethyl-C*H*$_2$), 3.17 (t, $^3J_{HH}$ = 4.9 Hz, 24H, ethyl-C*H*$_2$), 3.31 (sept, $^3J_{HH}$ = 6.8 Hz, 4H, ^{i}Pr-C*H*), 5.60 (s, 2H, quinone C*H*), 5.81 (d, $^3J_{HH}$ = 8.2 Hz, 6H, py *para-H*), 5.98 (t, $^3J_{HH}$ = 6.9 Hz, 6H, py *meta-H*), 7.10 (t, $^3J_{HH}$ = 6.9 Hz, 6H, py *meta-H*), 7.24 (t, $^3J_{HH}$ = 7.4 Hz, 2H, Dipp *para-H*), 7.32 (d, $^3J_{HH}$ = 7.6 Hz, 4H, Dipp *meta-H*), 8.01 (d, $^3J_{HH}$ = 4.3 Hz, 6H, py *ortho-H*). ^{13}C{^{1}H} NMR (175 MHz, d_5-pyridine, 300 K): δ_C / ppm 24.1 (^{i}Pr-*C*H$_3$), 26.1 (^{i}Pr-*C*H$_3$), 29.0 (^{i}Pr-*C*H), 46.2 (ethyl-*C*H$_2$), 55.4 (ethyl-*C*H$_2$), 101.1 (quinone *C*H), 103.9 (py *para-C*), 107.1 (py *meta-C*), 124.3 (Dipp, *meta-C*), 125.7 (Dipp *para-C*), 139.5 (py *meta-C*), 141.9 (Dipp, *ipso-C*-^{i}Pr), 145.5 (py *ortho-C*), 147.5 (Dipp *ipso-C*N), 167.0 (py *ipso-C*), 171.0 (quinone *C*N), 174.6 (quinone *C*O). Elemental analysis calculated for $C_{72}H_{84}N_{16}O_2Th_2$: C, 51.79 %; H, 5.07 %; N, 13.42 %. Found: C, 51.79 %; H, 4.92 %; N, 13.35

%. UV/vis (THF), λ / nm (ε / dm^3 mol^{-1} cm^{-1}): 268 (49,600), 365 (31,200).

Attempted synthesis of $[U(L)]_2Q^{Dipp}$ (4)

From $\mathbf{H_2Q^{Dipp}}$ (1 eq, 46 mg, 0.1 mmol) and **2** (2 eq, 0.2 mmol, 150 mg). ^{1}H NMR spectrum taken in $CDCl_3$ was uninformative and included several resonances between –13 and 55 ppm. (See SI, Figure S16)

Synthesis of $[Th(THF)(L)]_2Q^{OMe}$ (5)

From $\mathbf{H_2Q^{OMe}}$ (1 eq, 0.1 mmol, 35 mg) and **1** (1 eq, 0.1 mmol, 128 mg). Isolated as a microcrystalline red solid. Yield: 116 mg, 0.07 mmol (70%). ^{1}H NMR (500 MHz, d_5-pyridine, 300 K): δ_H / ppm 1.61 – 1.63 (m, 8H, THF), 2.81 (s, 12H, ethyl-CH_2), 3.17 (s, 12H, ethyl-CH_2), 3.47 (s, 6H, O-CH_3), 3.65 – 3-67 (m, 8H, THF), 5.68 (d, $^3J_{HH}$ = 8.4 Hz, 6H, py *meta-H*), 5.78 (s, 2H, quinone C*H*), 6.05 (t, $^3J_{HH}$ = 6.1 Hz, 6H, py *meta-H*), 6.86 (d, $^3J_{HH}$ = 7.8 Hz, 4H, anisidine *ortho-* and *meta-H*), 6.93 (t, $^3J_{HH}$ = 7.5 Hz, 2H, anisidine *para-H*), 7.12 – 7.07 (m, 8H, py *para-H* and anisidine *meta-H*), 8.07 (d, $^3J_{HH}$ = 4.6 Hz, 6H, py *ortho-H*). ^{13}C{^{1}H} NMR (125 MHz, C_6D_6, 300 K): δ_C / ppm 26.3 (THF), 45.6 (ethyl-*C*H_2), 54.2 (ethyl-*C*H_2), 55.5 (O-*C*H_3), 68.3 (THF), 98.2 (quinone *C*H), 103.4 (py *meta-C)*, 106.9 (py *meta-C*), 111.0 (anisidine *meta-C*), 120.6 (anisidine *para-C*), 125.5 (anisidine *ortho-C*), 138.8 (py *para-C*), 139.7 (anisidine *ipso-C*OCH_3), 145.1 (py *ortho-C)*, 152.0 (py *ipso-C*), 167.6 (anisidine *ipso-C*N), 169.0 (quinone *C*N), 176.2 (quinone *C*O). Elemental analysis calculated for $C_{70}H_{80}N_{16}O_6Th_2(C_4H_8O_1)$: C, 50.00 %; H, 4.99 %; N, 12.61 %. Found: C, 49.83 %; H, 5.13 %; N, 12.34 %. UV/vis (THF), λ / nm (ε / dm^3 mol^{-1} cm^{-1}): 244 (102,300), 271 (sh, 63,000), 305 (sh, 34,500), 354 (28,000), ca. 410 (sh, 18,500).

Synthesis of $[U(L)]_2Q^{OMe}$ (6)

From $\mathbf{H_2Q^{OMe}}$ (1 eq, 0.1 mmol, 35 mg) and **2** (2 eq, 0.2 mmol, 150 mg). Isolated as a microcrystalline brown solid. Yield: 100 mg, 0.062 mmol (62 %). ^{1}H NMR (600 MHz, d_5-pyridine, 300 K): δ_H / ppm –10.67 (s, broad, 4H, anisidine C*H*), –0.37 (s, 6H, py-*H*), 0.16 (s, 2H, anisidine C*H*), 1.92 (t, $^3J_{HH}$ = 9.2 Hz, py-*H*), 2.29 (s, 18H, ethyl-CH_2 and OCH_3), 2.72 (d, $^3J_{HH}$ = 7.92 Hz, 6H, py-*H*), 2.87 (t, $^3J_{HH}$ = 6.5 Hz, 2H, anisidine C*H*), 5.88 (s, broad, 14H, ethyl-CH_2 and quinone C*H*), 39.96 (s, 6H, py-*H*). Elemental analysis calculated for $C_{62}H_{64}N_{16}O_4U_2$: C, 47.69 %; H, 4.13 %; N, 14.35 %. Found: C, 47.31 %; H, 4.12 %; N, 14.50 %. UV/vis (THF), λ / nm (ε / dm^3 mol^{-1} cm^{-1}): 246 (82,800), 270 (sh, 29,000), 207 (25,800), 370 (28,800). Evans method magnetic moment: μ_{eff} = 3.88 μ_B.

Synthesis of $[K(18\text{-c-}6)(THF)_2][\{U(L)\}_2Q^{OMe}]$ (6^-)

A 3 mL THF solution of **6** (100 mg, 0.064 mmol, 1 eq) was frozen in a liquid-nitrogen cooled well in the glove box. A second, 2 mL THF slurry of KC_8 (10.3 mg, 0.076 mmol, 1.2 eq) was also frozen. The solution of **6** was added to the thawing KC_8 solution, and the mixture was allowed to warm to room temperature and then stirred at room temperature for 2 hours. Graphite was removed from the mixture by filtration through Celite® affording a dark red filtrate. 18-crown-6 ether (20.2 mg, 0.076 mmol, 1.2 eq) was added to the filtrate and stirred for 20 minutes at room temperature. The solution was then concentrated to *ca*. 1 mL and then stored at –40 °C to precipitate light red/brown solids. The solids were isolated by decanting the supernatant and drying under vacuum. Due to the extreme sensitivity of the complex, satisfactory elemental analysis could not be obtained. Light red/brown crystals suitable for single crystal X-ray diffraction studies were obtained from a THF solution stored at –40 °C.

Results and discussion

Halide-bearing actinide complexes of the tripodal ligand

The tripodal pyridyl-amine pro-ligand, tris[2-amino(2-pyridyl)-ethyl]amine, $\mathbf{H_3L}$, was prepared using a modified literature procedure and isolated as a yellow oil in high yield of 86 %. $\mathbf{H_3L}$ was deprotonated by a reaction with $K[N(SiMe_3)_2]$ in toluene, which afforded the potassium salt $\mathbf{K_3L}$, in 95 % yield as a light yellow powder (Scheme 2). The synthesis of $\mathbf{K_3L}$ was confirmed by ^{1}H NMR spectroscopy, which showed a loss of the N–H resonance (δ_H 5.29 ppm for $\mathbf{H_3L}$) and change in methylene proton chemical shifts. IR spectroscopy also showed a loss of N–H absorption bands in comparison with $\mathbf{H_3L}$.

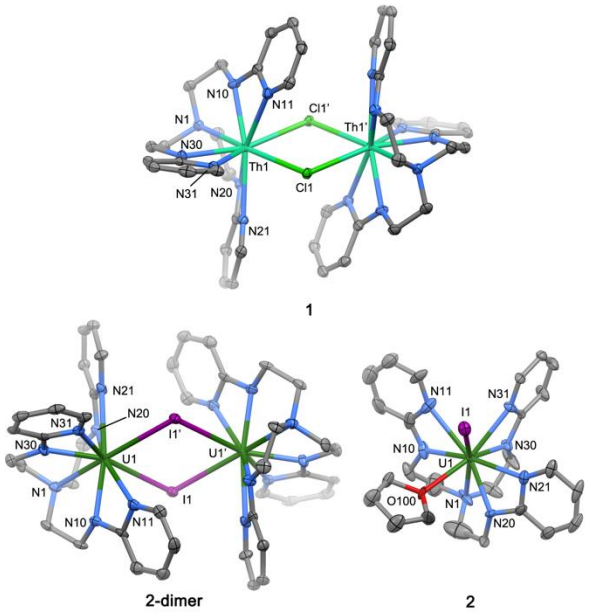

Figure 1. Solid-state structures of **1**, **2** and **2-dimer**. One half of the dimeric structures are symmetry-generated. For clarity, all protons are omitted and for **2**, a second molecule and 2.5 THF molecules present in the asymmetric unit are also omitted. Ellipsoids are drawn at 50 % probability.

Subsequent reaction of **K_3L** with $ThCl_4(DME)_2$ or $UI_4(dioxane)_2$ in THF led to the clean formation of the new complexes $[ThCl(L)]_2$ (**1**) and [UI(THF)(L)] (**2**), respectively (Scheme 2). X-ray quality crystals of **1** were obtained by vapour diffusion of hexane into a concentrated THF solution (Figure 1, top). The solid-state structure of **1** is dimeric, with the two thorium centres bridged asymmetrically by two chloride ligands (Th1–Cl1, 2.912(1) Å; Th1–Cl1', 2.948(1) Å), giving an intermetallic distance of 4.6124(4) Å. Each thorium centre is nine-coordinate, with N1 (the central amine), N30 and N31 (an amido-pyridyl chelating group) occupying the equatorial plane with the two bridging chloride ligands; the axial positions are each occupied by one of the remaining two bidentate amido-pyridyl groups. While the solution-state structure exhibits averaged C_3 symmetry, as judged by NMR spectroscopy, the solid-state structure reveals an asymmetric binding mode of the

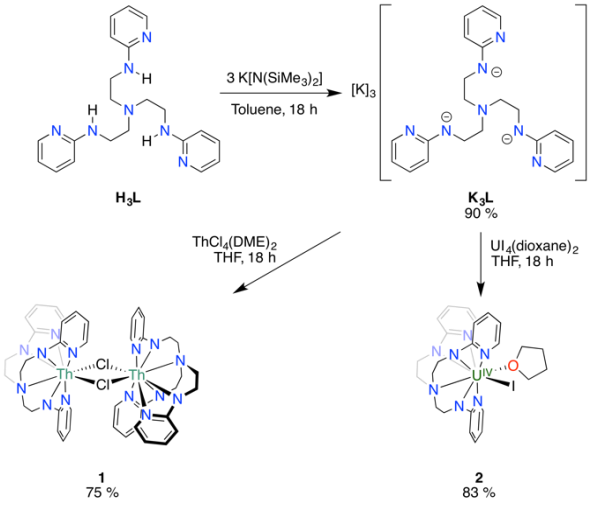

Scheme 2. Synthesis of **K_3L** from the deprotonation of **H_3L**, and subsequent synthesis of **1** and **2** from salt-metathesis reactions.

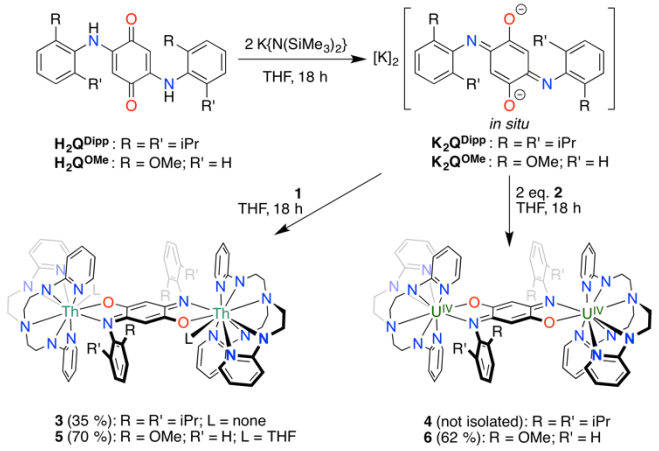

Scheme 3. Synthesis of the dinuclear, quinoid-bridged complexes of thorium (**3** and **5**) and of uranium(IV) (**4** and **6**), making use of the halide-bearing complexes **1** and **2** through salt-metathesis with deprotonated quinones **K_2Q^{Dipp}** and **K_2Q^{OMe}**.

tripodal ligand, where the amido-pyridyl chelating group containing N20 and N21 is twisted. Since this asymmetry is not resembled in the NMR spectra of the complexes, we attribute this to crystal packing effects.

The uranium complex **2** crystallised from a concentrated THF solution as a monomeric complex, in the triclinic space group P–1 (Figure 1, bottom right). The uranium centre is coordinated by all 7 nitrogen donor atoms from the tripodal ligand, along with one iodide and one THF ligand, giving a coordination number of nine. As for the crystal structure of **1**, the halide ligand in **2** is situated *trans* to the central amine nitrogen of the tripodal ligand. Due to THF coordination, the idealised C_{3v} symmetry imparted by the tripodal ligand is broken in the solid state, and the amido-pyridyl chelating group comprised of N20 and N21 appears distorted from its idealised position to accommodate the THF ligand.

Interestingly, single crystals grown from THF solutions of **2** layered with hexane are dimeric and isostructural to **1**, crystallising in the same space group of $P2_1/n$. Therefore, the dimerisation of **2** seems to occur only during crystallisation and is solvent-dependent. Just as for **1**, the two uranium(IV) centres

in **2-dimer** are also bridged asymmetrically by the two iodide ligands (U1–I1, 3.311(1) Å; U1–I1', 3.329(1) Å).

A diamagnetic ^{1}H NMR spectrum was obtained for **1** with resonances observed between δ_H 3.00 and 9.00 ppm in d_5-pyridine. In contrast, **2** showed paramagnetically shifted ^{1}H NMR resonances from δ_H 18.5 to –13.0 ppm, with the most characteristic being those at δ_H 17.4, 14.2, 11.2 and 9.3 ppm which correspond to the four inequivalent pyridyl protons. Interestingly, there are no NMR spectroscopic differences that imply formal "axial" and "equatorial" coordination of the tripodal ligand for **1** or **2** and the NMR spectra indicate averaged three-fold symmetry in solution. This is in stark contrast to previously reported complexes of tripodal ligands, for example ruthenium complexes of tris(2-pyridyl-methyl)amine display different sets of NMR resonances for the tripodal ligand corresponding to differences in equatorial *versus* axial coordination of the ligand arms.[25] The ^{1}H NMR spectrum of **2** showed the presence of three equivalents of free THF along with a single set of resonances for the complex. For the monomeric crystal structure, there are 2.5 equivalents of THF per molecule of **2** in the crystal lattice, with one THF bound, which agrees with the THF stoichiometry observed spectroscopically. Therefore, **2** is monomeric unless specifically crystallised from a THF/hexane mixture.

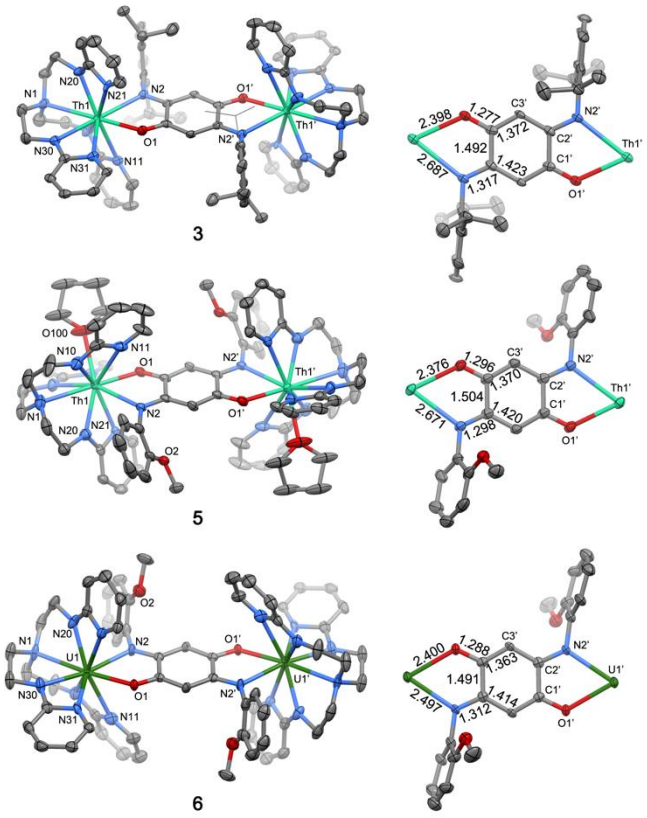

Figure 2. Left: Solid-state structures of **3**, **5** and **6**. For clarity, all protons are omitted. One molecule of THF present in the asymmetric unit of **5** is also omitted, along with a disordered methoxy group. Right: Magnified views of the M_2Q cores, showing important bond parameters within the quinoid bridge.

Quinoid-bridged actinide complexes

The amino-substituted quinones **H_2Q^{Dipp}** and **H_2Q^{OMe}** were deprotonated to give the corresponding quinoid anions **K_2Q^{Dipp}** and **K_2Q^{OMe}** using K[N(SiMe$_3$)$_2$] as base (Scheme 3). These potassium salts were not isolated, but reacted *in situ* with either **1** or **2** to yield dinuclear, quinoid-bridged complexes of thorium and uranium(IV), respectively.

The quinoid bridge with Dipp imino-substituents was successfully coordinated by two thorium centres, although the yield for [Th(L)]$_2$(Q^{Dipp}) (**3**) was low at 35 %. A full assignment of the ^{1}H and ^{13}C NMR resonances was made using 2D experiments and significant changes in chemical shifts were seen for all resonances attributed to the tripodal ligand in comparison with **1**.

Complex **3** crystallised from a concentrated THF solution in the C2/*c* space group (Figure 2, top). The tripodal ligand-to-metal bond distances in **3** are similar to those of **1**, with the exception of the central amine N1–Th1 distance, which is elongated by 0.12 Å in **3**. At 85.1°, the Dipp substituents on the bridging quinoid are nearly orthogonal to the plane of the quinoid.

Using the same procedure as for **3**, isolation of the targeted dinuclear uranium(IV) complex featuring the **Q^{Dipp}** bridging quinoid ([U(L)]$_2$(Q^{Dipp}), **4**) was not achieved. ^{1}H NMR spectra recorded of the crude material in d_5-pyridine featured several resonances between δ_H 55 and –13 ppm, but were largely uninformative (see Figure S16). No pure crystalline material could be isolated to study the uranium(IV) analogue of **3**.

Making use of the *ortho*-anisyl-substituted quinoid, **Q^{OMe}**, greatly improved the yield of the resulting dinuclear, bridged thorium complex [Th(L)]$_2$(Q^{OMe}) (**5**), which was isolated in 70 % yield (35 % for **3**). Furthermore, use of **Q^{OMe}** permitted clean formation of the uranium(IV) complex [U(L)]$_2$(Q^{OMe}) (**6**) and isolation in 62 % yield. ^{1}H NMR resonances for the tripodal ligand in **5** appeared at similar chemical shifts as for **3**. Resonances at δ_H 3.66 and 1.62 ppm are assigned to coordinated THF and their integrals suggest that one THF ligand is bound to each metal centre. For complex **6**, a number of broad, paramagnetically shifted resonances were observed between δ_H 40 and –11 ppm. It is interesting that the four resonances for the pyridyl groups span a wide range of chemical shift values, and were seen at δ_H 39.96, 2.72, 1.94 and –0.37 ppm. As for **3**, complexes **5** and **6** both have averaged C_3 symmetry in solution, with a single set of resonances seen for the tripodal ligand. This is despite the planar bridging ligand that is expected to break the symmetry and render the ligand protons inequivalent, as is observed with other other metal complexes with tripodal ligands and quinoid bridges.[26]

Single crystals of **5** were grown from a concentrated THF solution at –40 °C, while single crystals of **6** were obtained by vapour diffusion of hexane into a THF solution, and solid-state structures were determined for each by X-ray crystallography. In agreement with its ^{1}H NMR spectrum, complex **5** features a THF ligand coordinated to each thorium centre (Figure 2, middle). In contrast, the uranium complex **6** is free of solvent in the crystal lattice (Figure 2, bottom), presumably due to greater steric crowding within the uranium coordination sphere.

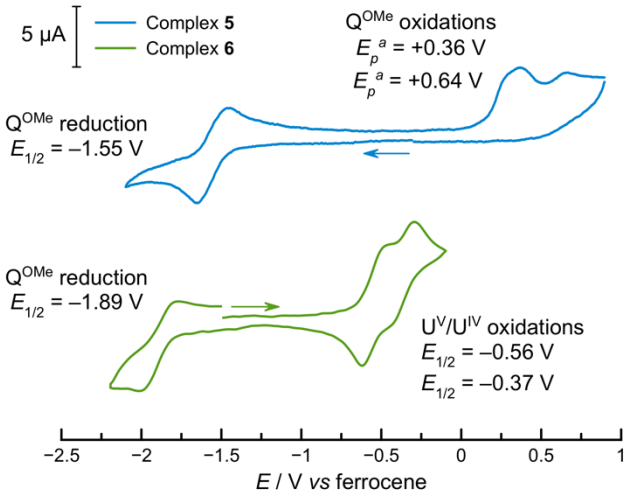

Figure 3. Cyclic voltammograms for the thorium complex **5** and the uranium(IV) complex **6**, measured at 100 mV s^{-1} in THF, using 0.1 M [^{n}Bu$_4$N][PF$_6$] as the supporting electrolyte. Pt-disc working electrode, Pt-wire quasi-reference electrode and Pt-gauze counter electrode.

Notably, whilst the thorium centre in **5** is able to accommodate an extra THF ligand, it does not employ the methoxy donor from the quinoid substituent.

At 63.9°, the anisyl quinoid substituents in **5** are not orthogonal to the bridge as in **3**. In the latter, an orthogonal arrangement was enforced because of the 2,6-substitution pattern on the Dipp groups. This twisting observed in **5** positions the methoxy groups in the centre of the bridge, above and below the quinoid plane. This twisting is also more pronounced in **5** than it is in **6**, where a torsion angle of 79.9° is seen. This is attributed to the larger ionic radius of thorium(IV) *versus* that of uranium(IV).[27]

Figure 2 summarises the important crystallographic bond distances within the quinoid bridges in complexes **3**, **5** and **6**. In all cases, the M–O1 bond distances are shorter than the M–N2 distances. Bearing in mind the strong oxophilicity of the early actinides, the quinoid ligand is perhaps best described as an imino-alkoxy ligand, with a stronger localisation of the negative charge on the oxygen donor.

Cyclic voltammetry

The electrochemical behaviour of the structurally-related complexes **5** and **6** was investigated by cyclic voltammetry (CV), using a three electrode setup with a Pt-disc working electrode in a 0.1 M THF solution of [^{n}Bu$_4$N][PF$_6$]. For the thorium quinoid complex **5**, a reversible reduction occurs at $E_{1/2}$ –1.55 V and irreversible oxidations occur at E_p^a +0.36 and +0.64 V, *versus* ferrocene (Figure 3). Given the redox inactivity of thorium within the electrochemical window of THF, these processes are one-electron redox events on the bridging quinoid ligand.

The uranium(IV) quinoid complex **6** showed three reversible redox processes in the CV (Figure 3). A one-electron reduction occurs at $E_{1/2}$ –1.89 V and two one-electron oxidations occur at $E_{1/2}$ –0.56 V and –0.37 V. As for **5**, the reduction of **6** is assigned to the formation of a quinoid radical-anion complex. The two oxidation processes occur at less positive potentials than that in

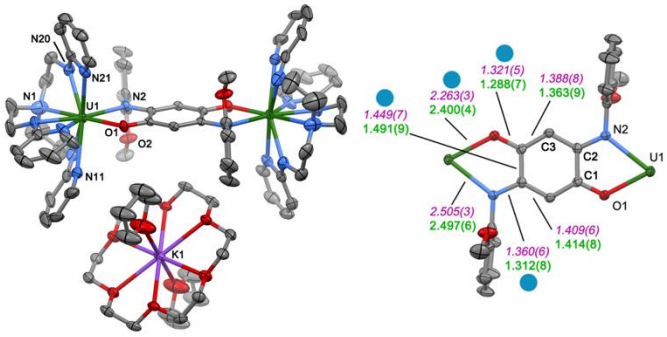

Figure 4. Left: Solid-state structure for **6**$^-$. For clarity, all protons and one molecule of THF in the asymmetric unit have been omitted. Thermal ellipsoids are drawn at 50 % probability. Right: focussed view of the U$_2$Q^{OMe} core, showing bond lengths for **6** in green (bold) and bond lengths for **6**$^-$ in pink (italics); changes in bond lengths that are significant beyond 3σ are highlighted with a blue spot.

5, and these are therefore assigned to reversible U(V)/U(IV) oxidations. The step-wise nature of the metal-centred oxidation does not necessarily indicate electronic communication between the two metal centres; it could instead be due to a geometric distortion in one of the tripodal ligand spheres following oxidation of the associated uranium centre, which perturbs the redox potential for the second uranium ion. Similar electrochemical behaviour has been reported for related cobalt(II) complexes, with a single quinoid-based reduction taking place along with step-wise metal-based oxidation.[1a, 1m]

Attempted chemical redox reactions with 6

The redox features observed in the CV of **6** indicate that reduced, singly-oxidised (mixed-valent) and doubly-oxidised complexes may be chemically accessible. Attempts were made to isolate **6**$^+$ and **6**$^{2+}$ from oxidation reactions with [Ag][OTf], [Ag][BPh$_4$], [FeCp$_2$][BPh$_4$] and [FeCp$_2$][PF$_6$]. It was evident that oxidation reactions had occurred; for example, Ag metal was deposited from reactions involving Ag(I), and from reactions with [FeCp$_2$][BPh$_4$], the FeCp$_2$ ^{1}H NMR resonance was observed at δ_H 4.15 ppm (CD_2Cl_2) along with those for [BPh$_4$]$^-$ at δ_H 7.50, 7.18 and 7.00 ppm. However, the NMR resonances for the rest of the complex were uninformative, and pure material could not be isolated from attempted crystallisations.

As discussed above, dinuclear complexes bridged by a radical, π-conjugated ligand are desirable compounds for studying intermetallic exchange interactions and SMM. It has also been shown previously that radical-containing ligands promote SMM behaviour in the absence of an applied magnetic field, as the local magnetic moment from the unpaired electron maintains non-degeneracy in the m_J levels.[28] Therefore, our main synthetic target was therefore **6**$^-$ and we found that chemical reduction was achieved using KC_8 in thawing THF. After removal of graphite by filtration, 18-crown-6 ether was added to promote crystallisation of the potassium salt of **6**$^-$. Whilst a small number of single crystals were isolated from a THF solution of **6**$^-$ cooled to –40 °C and studied by X-ray crystallography, satisfactory elemental analysis for the bulk material could not be obtained. This reaction was repeated multiple times, but changes to the reaction solvent (diethyl

ether), chelating agent (2.2.2-cryptand) or reaction time did not improve the purity of the product. Unfortunately, this has precluded a more detailed investigation into the electronic structure of **6**$^{-}$ by magnetometry. Whilst attempts were made to investigate the radical nature of the reduced complex by X-band EPR spectroscopy (in the solid state and in frozen solution), the spectra recorded from three separate batches were inconsistent. The lack of purity is attributed to thermal instability and high sensitivity of the complex to adventitious moisture and oxygen.

In the X-ray crystal structure of **6**$^{-}$, the tripodal ligands are positioned away from the bridging region, with all of the nitrogen donor atoms inhabiting one half of the uranium coordination sphere (Figure 4). This is probably due to crystal packing as the $[K(18\text{-c-}6)(THF)_2]^+$ cation is located between the two capping tripodal ligands. A one-electron reduction is inferred from the 1:1 ratio between **6**$^{-}$ and K^+ in the asymmetric unit. Comparing the changes in bond lengths between **6** and **6**$^{-}$ (those that are statistically significant beyond 3σ) indicate that a ligand-based reduction takes place. The U1–O1 bond length contracts by 0.137 Å upon reduction, which is not indicative of a lowering of the metal's formal oxidation state on the metal. In contrast, the quinoid C1–O1 and C2–N2 bond lengths both increase by 0.033 Å and 0.048 Å, respectively, whilst the C1–C2 bond contracts by 0.042 Å. DFT calculations carried out for **6** show that one of the four singly-occupied molecular orbitals (SOMO–2) has significant quinoid ligand character and describes a π-anti-bonding interaction for C1–O1 and C2–N2, as well as a π-bonding interaction for C1–C2 (Figure S58). The observed changes in quinoid bond lengths therefore agree with increased electron density at the quinoid bridge and the formation of a ligand-centred radical.

The four unpaired electrons for **6** occupy SOMOs that are mainly of mixed uranium/quinoid character (only SOMO–1 is purely metal-based), the unpaired spin-density plot shows that there is significant spin-delocalisation from uranium to the quinoid.

A comparison of the calculated free-energies for the quartet and sextet spin-states of **6**$^{-}$ indicate that the quartet is preferred, as it is 16 kcal mol^{-1} lower in energy than the sextet. This indicates that the reduction of **6** also leads to spin-pairing with an unpaired electron on **6**, lowering the multiplicity. The three SOMOs for **6**$^{-}$ are also mainly of mixed uranium/quinoid character, although SOMO–2 is practically purely metal-based. The spin-density plot for **6**$^{-}$ appears similar to **6** and shows significant localisation of the spin density on the uranium centres. However, the spin-density difference-plot {ρ(**6**$^{-}$) – ρ(**6**)} reveals that the extra electron-density in the anionic complex is located purely on the quinoid, in agreement with the changes in bond lengths discussed above.

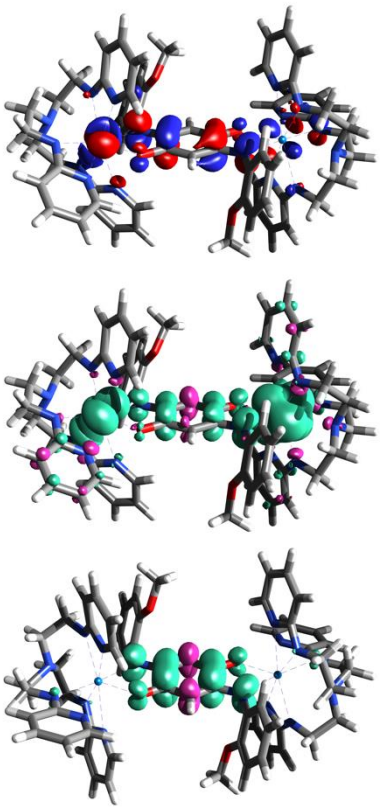

Figure 5. Top: SOMO–2 for **6**, highlighting the mixed uranium/quinoid character in the frontier molecular orbitals; the π-bonding interactions in the quinoid ligand complement the observed bond changes in Figure 4. Middle: unpaired spin-density for **6**, showing spin-delocalisation to the formally diamagnetic quinoid bridge. Bottom: spin-density difference-plot, {ρ(6–) – ρ(6)}, further supporting that **6**$^{-}$ contains a radical-quinoid bridge. Calculated using the B3PW91 functional, ECP78MWB pseudo-potential (along with its adapted basis set) for uranium, and 6-31G(d,p) basis set for light atoms; all surfaces displayed with an iso-value of 0.02.

Magnetic investigation of 2 and 6

Variable temperature DC magnetic susceptibility measurements for **2-dimer** provide a room-temperature (300 K) χT value of 1.91 emu K mol^{-1} at 5000 Oe (μ_{eff} = 3.91 μ_B), which is well below that expected for two isolated, free-ion uranium(IV) centres (3.2 emu K mol^{-1}). Similarly, the room temperature χT value for **6** was 2.22 emu K mol^{-1} at 1000 Oe (μ_{eff} = 4.21 μ_B). These values are within the range of those reported for other uranium(IV) mono- and di-nuclear complexes.[29] Their deviation from the expected values is ascribed to ligand-field splitting of the *J* ground-state multiplets.

For comparison, the room-temperature, solution-phase magnetic moments for **2** and **6** were measured using the Evans NMR method.[30] For **2**, which is monomeric in solution, μ_{eff} = 2.85 μ_B and is lower than that predicted by the Landé formula for a single free uranium(IV) ion (3.58 μ_B).[31] For **6**, μ_{eff} = 3.88 μ_B, which is slightly lower than that measured in the solid state.

As the temperature is decreased, the susceptibility for **2-dimer** decreases, from 1.91 emu K mol^{-1} to 0.05 emu K mol^{-1} at 2 K; the same value was measured for **6** at 2 K (Figure 6). Reduction of the susceptibility and moment at lower

temperatures is typical for uranium(IV) ($5f^2$) complexes and is consistent with a poorly isolated singlet ground-state arising from crystal field effects.[29] The low-temperature susceptibility data indicates that the ground states for **2-dimer** and **6** are non-magnetic singlets that are not well isolated. Magnetic behaviour at higher temperature is therefore due to excited paramagnetic states as well as temperature-independent paramagnetism.

If any magnetic coupling exists between the two uranium(IV) centres in **2-dimer** or **6**, it is incredibly weak and cannot be quantified from the DC susceptibility measurements. At low temperature, χT is strongly influenced by partial quenching of the orbital angular momentum by the ligand field. The long intermetallic distances, at 5.125(1) Å for **2-dimer** and 8.904(1) Å for **6**, further support the likelihood that any magnetic coupling in these systems would be negligible.

Summary

The thorium and uranium derivatives of the tripodal tris[2-amido(2-pyridyl)ethyl]amine ligand **L**, bearing ancillary halide ligands, are precursors to novel quinoid-bridged dinuclear actinide complexes. Whilst the thorium complex of the bridging $\mathbf{Q^{Dipp}}$ ligand was isolated, better yields were obtained using the $\mathbf{Q^{OMe}}$ ligand, and the uranium species was only isolated using this latter quinoid bridge, showing that the quinoid N-substituents are important in terms of synthesis. Despite its chelating nature, the tripodal supporting ligand is quite flexible and adopts different positions in the coordination sphere in order to accommodate different bridging ligands and cations located between the two metal centres. Both thorium and uranium(IV) ions make use of all seven donor atoms from the tripodal ligand, resulting in high coordination numbers in the complexes.

Both the thorium and uranium complexes **5** and **6** display reversible redox activity in their cyclic voltammograms indicating that the quinoid ligand undergoes reversible reduction to form a radical anion. However, chemical redox reactions with **6** were not straightforward, and chemical reduction of **6** with KC_8 leads to an unstable and sensitive complex, and X-ray crystallography indicates that the product contains a radical bridge.

Magnetometry measurements for **2-dimer** and **6** show that despite the iodide and quinoid bridges between the uranium(IV) ions, magnetic coupling between the two metals is negligible. Unfortunately, due to a lack of bulk purity for $\mathbf{6^-}$, its magnetometry has not been studied and the impact of the radical bridge on the intermetallic exchange interaction cannot be determined. In the future we will extend our studies towards other bridging ligands which may allow for a higher degree of coupling in their neutral from, and offer higher stabilities in their singly reduced forms to study possible intermetallic exchange interactions.

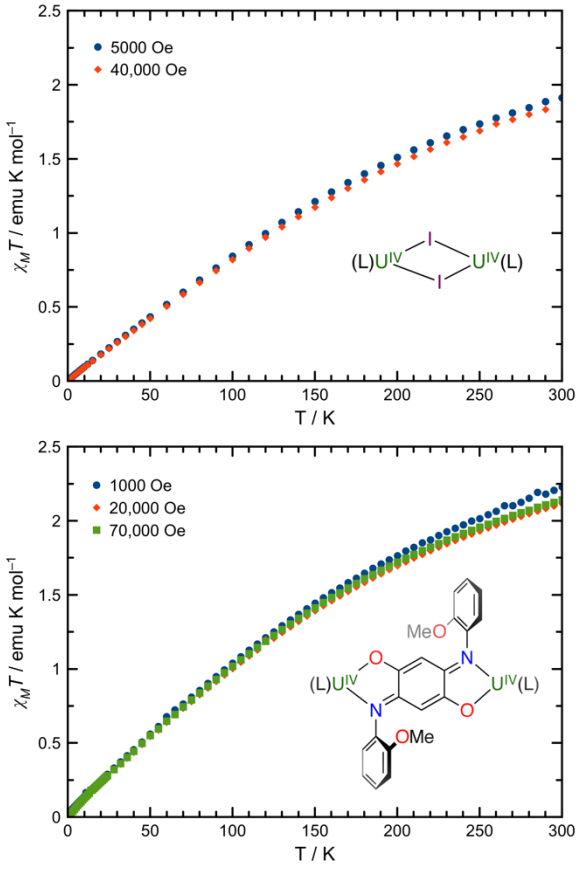

Figure 6. Variable-temperature DC magnetic susceptibility data for **2-dimer** (top) and **6** (bottom).

Acknowledgements

J.R.P. thanks the University of Edinburgh for funding a research visit to UC Berkeley and LBNL through a ScotCHEM International Graduate School Scholarship. S.H. acknowledges the German Academic Exchange Service (DAAD) for a postdoctoral scholarship. E.E.J. gratefully acknowledges financial support from the German Academic Exchange Service (DAAD) through its Thematic Network "ACalNet" funded by the German Federal Ministry of Education and Research (BMBF). M.E.G. acknowledges the NSF-GRFP (CHE-0840505) for a graduate research fellowship. This work was supported by the Director, Office of Science, Office of Basic Energy Sciences, Division of Chemical Sciences, Geosciences, and Biosciences Heavy Element Chemistry Program of the U.S. Department of Energy (DOE) at LBNL under Contract No. DE-AC02-05CH11231. Furthermore, we also would like to thank the NIH (Grant S10-RR027172) for financial support of our X-Ray crystallographic facility. We thank Prof. Jeffrey Long (UC Berkeley) for use of his SQUID magnetometer and Dr Guodong Rao (UC Davis) for EPR spectroscopy. Nick S. Settineri, Michael A. Boreen and Trevor D. Lohrey, are kindly acknowledged for helpful discussion.

Notes and references

1. (a) M. van der Meer, Y. Rechkemmer, U. Frank, F. D. Breitgoff, S. Hohloch, C.-Y. Su, P. Neugebauer, R. Marx, M. Dörfel, J. van Slageren and B. Sarkar, *Chem. Eur. J.*, 2016, **22**, 13884; (b) B. Sarkar, D. Schweinfurth, N. Deibel and F. Weisser, *Coord. Chem. Rev.*, 2015, **293–294**, 250; (c) M. G. Sommer, D. Schweinfurth, F. Weisser, S. Hohloch and B. Sarkar, *Organometallics*, 2013,

32, 2069; (d) H. S. Das, F. Weisser, D. Schweinfurth, C.-Y. Su, L. Bogani, J. Fiedler and B. Sarkar, *Chem. Eur. J.*, 2010, **16**, 2977; (e) S. Kar, B. Sarkar, S. Ghumaan, D. Janardanan, J. van Slageren, J. Fiedler, V. G. Puranik, R. B. Sunoj, W. Kaim and G. K. Lahiri, *Chem. Eur. J.*, 2005, **11**, 4901; (f) D. Gupta, V. Singh, S. Hohloch, M. Sathiyendiran, K. Tedin and B. Sarkar, *Polyhedron*, 2015, **100**, 243; (g) H. S. Das, D. Schweinfurth, J. Fiedler, M. M. Khusniyarov, S. M. Mobin and B. Sarkar, *Chem. Eur. J.*, 2014, **20**, 4334; (h) N. Deibel, S. Hohloch, D. Schweinfurth, F. Weisser, A. Grupp and B. Sarkar, *Chem. Eur. J.*, 2014, **20**, 15178; (i) N. Deibel, M. G. Sommer, S. Hohloch, J. Schwann, D. Schweinfurth, F. Ehret and B. Sarkar, *Organometallics*, 2014, **33**, 4756; (j) I.-R. Jeon, L. Sun, B. Negru, R. P. Van Duyne, M. Dincă and T. D. Harris, *J. Am. Chem. Soc.*, 2016, **138**, 6583; (k) A. Paretzki, H. S. Das, F. Weisser, T. Scherer, D. Bubrin, J. Fiedler, J. E. Nycz and B. Sarkar, *Eur. J. Inorg. Chem.*, 2011, **2011**, 2413; (l) J. G. Park, I.-R. Jeon and T. D. Harris, *Inorg. Chem.*, 2015, **54**, 359; (m) D. Schweinfurth, Y. Rechkemmer, S. Hohloch, N. Deibel, I. Peremykin, J. Fiedler, R. Marx, P. Neugebauer, J. van Slageren and B. Sarkar, *Chem. Eur. J.*, 2014, **20**, 3475; (n) D. Schweinfurth, J. Klein, S. Hohloch, S. Dechert, S. Demeshko, F. Meyer and B. Sarkar, *Dalton Trans.*, 2013, **42**, 6944; (o) D. Schweinfurth, H. S. Das, F. Weisser, D. Bubrin and B. Sarkar, *Inorg. Chem.*, 2011, **50**, 1150; (p) M. Yuan, F. Weisser, B. Sarkar, A. Garci, P. Braunstein, L. Routaboul and B. Therrien, *Organometallics*, 2014, **33**, 5043.

2. A. I. Gaudette, I.-R. Jeon, J. S. Anderson, F. Grandjean, G. J. Long and T. D. Harris, *J. Am. Chem. Soc.*, 2015, **137**, 12617.
3. D. Schweinfurth, M. M. Khusniyarov, D. Bubrin, S. Hohloch, C.-Y. Su and B. Sarkar, *Inorg. Chem.*, 2013, **52**, 10332.
4. M. van der Meer, Y. Rechkemmer, F. D. Breitgoff, R. Marx, P. Neugebauer, U. Frank, J. van Slageren and B. Sarkar, *Inorg. Chem.*, 2016, **55**, 11944.
5. C. Carbonera, A. Dei, J.-F. Létard, C. Sangregorio and L. Sorace, *Angew. Chem. Int. Ed.*, 2004, **43**, 3136.
6. I.-R. Jeon, J. G. Park, D. J. Xiao and T. D. Harris, *J. Am. Chem. Soc.*, 2013, **135**, 16845.
7. S. Demir, I.-R. Jeon, J. R. Long and T. D. Harris, *Coord. Chem. Rev.*, 2015, **289–290**, 149.
8. (a) N. H. Anderson, S. O. Odoh, U. J. Williams, A. J. Lewis, G. L. Wagner, J. Lezama Pacheco, S. A. Kozimor, L. Gagliardi, E. J. Schelter and S. C. Bart, *J. Am. Chem. Soc.*, 2015, **137**, 4690; (b) C. Camp, V. Mougel, P. Horeglad, J. Pécaut and M. Mazzanti, *J. Am. Chem. Soc.*, 2010, **132**, 17374; (c) P. L. Diaconescu and C. C. Cummins, *Dalton Trans.*, 2015, **44**, 2676; (d) J. J. Kiernicki, D. P. Cladis, P. E. Fanwick, M. Zeller and S. C. Bart, *J. Am. Chem. Soc.*, 2015, **137**, 11115; (e) J. J. Kiernicki, B. S. Newell, E. M. Matson, N. H. Anderson, P. E. Fanwick, M. P. Shores and S. C. Bart, *Inorg. Chem.*, 2014, **53**, 3730; (f) S. J. Kraft, P. E. Fanwick and S. C. Bart, *J. Am. Chem. Soc.*, 2012, **134**, 6160; (g) S. J. Kraft, U. J. Williams, S. R. Daly, E. J. Schelter, S. A. Kozimor, K. S. Boland, J. M. Kikkawa, W. P. Forrest, C. N. Christensen, D. E. Schwarz, P. E. Fanwick, D. L. Clark, S. D. Conradson and S. C. Bart, *Inorg. Chem.*, 2011, **50**, 9838; (h) S. J. Kraft, P. E. Fanwick and S. C. Bart, *Inorg. Chem.*, 2010, **49**, 1103; (i) E. M. Matson, S. R. Opperwall, P. E. Fanwick and S. C. Bart, *Inorg. Chem.*, 2013, **52**, 7295; (j) S. A. Pattenaude, C. S. Kuehner, W. L. Dorfner, E. J. Schelter, P. E. Fanwick and S. C. Bart, *Inorg. Chem.*, 2015, **54**, 6520; (k) S. Fortier, J. Veleta, A. Pialat, J. Le Roy, K. B. Ghiassi, M. M. Olmstead, A. Metta-Magaña, M. Murugesu and D. Villagrán, *Chem. Eur. J.*, 2016, **22**, 1931.
9. J. D. Rinehart, M. Fang, W. J. Evans and J. R. Long, *Nat. Chem.*, 2011, **3**, 538.
10. S. Demir, M. Nippe, M. I. Gonzalez and J. R. Long, *Chem. Sci.*, 2014, **5**, 4701.
11. F.-S. Guo and R. A. Layfield, *Chem. Commun.*, 2017, **53**, 3130.
12. B. S. Dolinar, S. Gomez-Coca, D. I. Alexandropoulos and K. R. Dunbar, *Chem. Commun.*, 2017, **53**, 2283.
13. F. Pointillart, B. Le Guennic, T. Cauchy, S. Golhen, O. Cador, O. Maury and L. Ouahab, *Inorg. Chem.*, 2013, **52**, 5978.
14. (a) F. Pointillart, S. Klementieva, V. Kuropatov, Y. Le Gal, S. Golhen, O. Cador, V. Cherkasov and L. Ouahab, *Chem. Commun.*, 2012, **48**, 714; (b) F. Pointillart, V. Kuropatov, A. Mitin, O. Maury, Y. Le Gal, S. Golhen, O. Cador, V. Cherkasov and L. Ouahab, *Eur. J. Inorg. Chem.*, 2012, **2012**, 4708.
15. (a) K. R. Meihaus and J. R. Long, *Dalton Trans.*, 2015, **44**, 2517; (b) K. R. Meihaus, S. G. Minasian, W. W. Lukens, S. A. Kozimor, D. K. Shuh, T. Tyliszczak and J. R. Long, *J. Am. Chem. Soc.*, 2014, **136**, 6056; (c) J. D. Rinehart and J. R. Long, *Dalton Trans.*, 2012, **41**, 13572; (d) K. R. Meihaus, J. D. Rinehart and J. R. Long, *Inorg. Chem.*, 2011, **50**, 8484; (e) J. D. Rinehart, K. R. Meihaus and J. R. Long, *J. Am. Chem. Soc.*, 2010, **132**, 7572; (f) J. D. Rinehart and J. R. Long, *J. Am. Chem. Soc.*, 2009, **131**, 12558; (g) S. T. Liddle and J. van Slageren, *Chem. Soc. Rev.*, 2015, **44**, 6655; (h) F. Moro, D. P. Mills, S. T. Liddle and J. van Slageren, *Angew. Chem. Int. Ed.*, 2013, **52**, 3430; (i) C. A. P. Goodwin, F. Tuna, E. J. L. McInnes, S. T. Liddle, J. McMaster, I. J. Vitorica-Yrezabal and D. P. Mills, *Chem. Eur. J.*, 2014, **20**, 14579; (j) J. T. Coutinho, M. A. Antunes, L. C. J. Pereira, H. Bolvin, J. Marcalo, M. Mazzanti and M. Almeida, *Dalton Trans.*, 2012, **41**, 13568; (k) M. A. Antunes, L. C. J. Pereira, I. C. Santos, M. Mazzanti, J. Marçalo and M. Almeida, *Inorg. Chem.*, 2011, **50**, 9915.
16. (a) P. L. Arnold, G. M. Jones, S. O. Odoh, G. Schreckenbach, N. Magnani and J. B. Love, *Nat. Chem.*, 2012, **4**, 221; (b) O. P. Lam, F. W. Heinemann and K. Meyer, *Chem. Sci.*, 2011, **2**, 1538.
17. B. M. Gardner, D. M. King, F. Tuna, A. J. Wooles, N. F. Chilton and S. T. Liddle, *Chem. Sci.*, 2017, DOI: 10.1039/C7SC01998J.
18. D. P. Mills, F. Moro, J. McMaster, J. van Slageren, W. Lewis, A. J. Blake and S. T. Liddle, *Nat. Chem.*, 2011, **3**, 454.
19. R. K. Rosen, R. A. Andersen and N. M. Edelstein, *J. Am. Chem. Soc.*, 1990, **112**, 4588.
20. B. S. Newell, A. K. Rappé and M. P. Shores, *Inorg. Chem.*, 2010, **49**, 1595.
21. (a) P. Roussel, N. W. Alcock, R. Boaretto, A. J. Kingsley, I. J. Munslow, C. J. Sanders and P. Scott, *Inorg. Chem.*, 1999, **38**, 3651; (b) P. Roussel, N. D. Tinker and P. Scott, *J. Alloys Compd.*, 1998, **271–273**, 150; (c) P. Roussel, P. B. Hitchcock, N. D. Tinker and P. Scott, *Inorg. Chem.*, 1997, **36**, 5716; (d) P. Scott and P. B. Hitchcock, *J. Chem. Soc., Dalton Trans.*, 1995, DOI: 10.1039/DT9950000603, 603; (e) E. P. Wildman, J. P. A. Ostrowski, D. M. King, W. Lewis and S. T. Liddle, *Polyhedron*, 2017, **125**, 2; (f) J. L. Brown, A. J. Gaunt, D. M. King, S. T. Liddle, S. D. Reilly, B. L. Scott and A. J. Wooles, *Chem. Commun.*, 2016, **52**, 5428; (g) B. M. Gardner and S. T. Liddle, *Chem. Commun.*, 2015, **51**, 10589; (h) B. M. Gardner, G. Balázs, M. Scheer, A. J. Wooles, F. Tuna, E. J. L. McInnes, J. McMaster, W. Lewis, A. J. Blake and S. T. Liddle, *Angew. Chem. Int. Ed.*, 2015, **54**, 15250; (i) B. M. Gardner, F. Tuna, E. J. L. McInnes, J. McMaster, W. Lewis, A. J. Blake and S. T. Liddle, *Angew. Chem. Int. Ed.*, 2015, **54**, 7068; (j) B. M. Gardner, G. Balázs, M. Scheer, F. Tuna, E. J. L. McInnes, J. McMaster, W. Lewis, A. J. Blake and S. T. Liddle, *Angew. Chem. Int. Ed.*, 2014, **53**, 4484; (k) P. A. Cleaves, D. M. King, C. E. Kefalidis, L. Maron, F. Tuna, E. J. L. McInnes, J. McMaster, W. Lewis, A. J. Blake and S. T. Liddle, *Angew. Chem. Int. Ed.*, 2014, **53**, 10412; (l) B. M. Gardner, P. A. Cleaves, C. E. Kefalidis, J. Fang, L. Maron, W. Lewis, A. J. Blake and S. T. Liddle, *Chem. Sci.*, 2014, **5**, 2489; (m) D. M. King, F. Tuna, E. J. L. McInnes, J. McMaster, W. Lewis, A. J. Blake and S. T. Liddle, *Nat. Chem.*, 2013, **5**, 482; (n) B. Kosog, H. S. La Pierre, F. W. Heinemann, S. T. Liddle and K. Meyer, *J. Am. Chem. Soc.*, 2012, **134**, 5284; (o) B. M. Gardner, J. C. Stewart, A. L. Davis, J. McMaster, W. Lewis, A. J. Blake and S. T. Liddle, *Proceedings of the National Academy of Sciences*, 2012, **109**, 9265; (p) B. M. Gardner, D. Patel, W. Lewis, A. J. Blake and S. T. Liddle, *Angew. Chem. Int. Ed.*, 2011, **50**, 10440; (q) S. T. Liddle, J. McMaster, D. P. Mills, A. J. Blake, C. Jones and W. D. Woodul, *Angew. Chem. Int. Ed.*, 2009, **48**, 1077; (r) B. M. Gardner, J. McMaster, W. Lewis, A. J. Blake and S. T. Liddle, *Journal of the American Chemical Society*, 2009, **131**, 10388; (s) B. M. Gardner, J. McMaster, W. Lewis and S. T. Liddle, *Chemical Communications*, 2009, DOI: 10.1039/B906554G, 2851.
22. (a) J. Hümmer, F. W. Heinemann and K. Meyer, *Inorg. Chem.*, 2017, **56**, 3201; (b) D. P. Halter, F. W. Heinemann, J. Bachmann and K. Meyer, *Nature*, 2016, **530**, 317; (c) A.-C. Schmidt, F. W. Heinemann, W. W. Lukens and K. Meyer, *J. Am. Chem. Soc.*, 2014, **136**, 11980; (d) S. M. Franke, F. W. Heinemann and K. Meyer, *Chem. Sci.*, 2014, **5**, 942; (e) H. S. La Pierre and K. Meyer, *Inorg. Chem.*, 2013, **52**, 529; (f) O. P. Lam, S. M. Franke, H. Nakai, F. W. Heinemann, W. Hieringer and K. Meyer, *Inorg. Chem.*, 2012, **51**, 6190; (g) A.-C. Schmidt, A. V. Nizovtsev, A. Scheurer, F. W. Heinemann and K. Meyer, *Chem. Commun.*, 2012, **48**, 8634; (h) S. J. Zuend, O. P. Lam, F. W. Heinemann and K. Meyer, *Angew. Chem. Int. Ed.*, 2011, **50**, 10626; (i) S. C. Bart, F. W. Heinemann, C. Anthon, C. Hauser and K. Meyer, *Inorg. Chem.*, 2009, **48**, 9419; (j) O. P. Lam, P. L. Feng, F. W. Heinemann, J. M. O'Connor and K. Meyer, *Journal of the American Chemical Society*, 2008, **130**, 2806; (k) S. C. Bart, C. Anthon, F. W. Heinemann, E. Bill, N. M. Edelstein and K. Meyer, *Journal of the American Chemical Society*, 2008, **130**, 12536; (l) I. Castro-Rodríguez, H. Nakai and K. Meyer, *Angewandte Chemie*, 2006, **118**, 2449; (m) I. Castro-Rodriguez and K. Meyer, *Journal of the American Chemical Society*, 2005, **127**, 11242; (n) I. Castro-Rodriguez, H. Nakai, L. N. Zakharov, A. L. Rheingold and K. Meyer, *Science*, 2004, **305**, 1757; (o) I. Castro-Rodriguez, K. Olsen, P. Gantzel and K. Meyer, *J. Am. Chem. Soc.*, 2003, **125**, 4565; (p) I. Castro-Rodriguez, H. Nakai, P. Gantzel, L. N. Zakharov, A. L. Rheingold and K. Meyer, *Journal of the American Chemical Society*, 2003, **125**, 15734; (q) I. Castro-Rodriguez, K. Olsen, P. Gantzel and K. Meyer, *Chemical Communications*, 2002, DOI: 10.1039/B208473B, 2764.
23. A. L. Ward, W. W. Lukens, C. C. Lu and J. Arnold, *J. Am. Chem. Soc.*, 2014, **136**, 3647.
24. S. J. Tereniak, R. K. Carlson, L. J. Clouston, V. G. Young, E. Bill, R. Maurice, Y.-S. Chen, H. J. Kim, L. Gagliardi and C. C. Lu, *J. Am. Chem. Soc.*, 2014, **136**, 1842.
25. T. Kojima, T. Amano, Y. Ishii, M. Ohba, Y. Okaue and Y. Matsuda, *Inorg. Chem.*, 1998, **37**, 4076.
26. F. Weisser, R. Huebner, D. Schweinfurth and B. Sarkar, *Chem. Eur. J.*, 2011, **17**, 5727.
27. R. Shannon, *Acta Crystallogr. Sect. A*, 1976, **32**, 751.
28. (a) M. A. Antunes, J. T. Coutinho, I. C. Santos, J. Marçalo, M. Almeida, J. J. Baldoví, L. C. J. Pereira, A. Gaita-Ariño and E. Coronado, *Chem. Eur. J.*, 2015, **21**, 17817; (b) J. T. Coutinho, M. A. Antunes, L. C. J. Pereira, J. Marcalo and M. Almeida, *Chem. Commun.*, 2014, **50**, 10262.
29. (a) N. M. Edelstein and G. H. Lander, *The Chemistry of the Actinide and Transactinide Elements*, Springer: Dordrecht, The Netherlands, 3rd edn., 2006; (b) B. Kanellakopulos, *Organometallics of the f-Elements*, D. Reidel

Pub. Co.: Dordrecht, The Netherlands, 1978; (c) T. H. Siddall, *Theory and Applications of Molecular Paramagnetism*, Wiley: New York, 1976.
30. (a) E. M. Schubert, *J. Chem. Ed.*, 1992, **69**, 62; (b) D. F. Evans, *J. Chem. Soc.*, 1959, 2003.
31. S. T. Liddle, *Angew. Chem. Int. Ed.*, 2015, **54**, 8604.